LABORATORI NAZIONALI DI FRASCATI
SIS – Pubblicazioni

LNF–03/002 (IR)
18 Febbraio 2003

SYNCHROTRON RADIATION FROM DAΦNE BENDING MAGNET AND WIGGLER

Irina Titkova [1], Mikhail Zobov [2], Sultan Dabagov [2,3]

[1)] *Joint Institute for Nuclear Research, Dubna, Russia*
[2)] *INFN-Laboratori Nazionali di Frascati, I-00044 Frascati, Italy*
[3)] *RAS – P.N. Lebedev Physical Institute, 119991 Moscow, Russia*

Abstract

DAΦNE is a special kind of accelerator dedicated to the production of Φ-particles coming from the annihilation of electrons and positrons at the Φ-resonance energy. However, due to the very large circulating current, DAΦNE represents also a high flux source of synchrotron radiation in the infrared and soft X-ray wavelength region. In this paper the main characteristics of synchrotron radiation from DAΦNE's wigglers and dipole magnets are estimated for the parasitic regime of operation. The results of calculations for KLOE and DEAR lattices have been compared.

PACS.: 41.60.Ap; 07.85.Qe

1 INTRODUCTION

The optics of DAΦNE is adopted to satisfy high intensity and high luminosity requirements. In order to achieve a required luminosity a double ring scheme has been chosen [1-4]. Beam-beam interaction sets limits to the maximum achievable luminosity that is severe at low energy. In this case the radiation damping and noise are strong parameters in determining the luminosity. In order to increase the energy radiated, four normal conducting wigglers were installed in the Main Ring lattice. As well-known, wiggler is a source of synchrotron radiation (SR). However, the DAΦNE wigglers are mainly used for the emittance control, which is very important parameter for the beam-beam interaction that allows the luminosity to be essentially improved. On the other hand, the characteristics of SR are defined by the parameters of wiggler, namely, for the best radiation parameters the low betas and zero dispersion functions are needed in the wiggler locations. Hence, synchrotron light from the DAΦNE wigglers can be used only in a parasitic mode of operation.

The main goal of this paper is to estimate characteristics and parameters of SR from the DAΦNE wigglers and dipole magnets for the main regimes of operation and to compare how the SR brightness is changed while passing from one experimental lattice to another. For this purpose we compare the results of calculations for the KLOE and DEAR lattices.

2 SYNCHROTRON RADIATION FROM BENDING MAGNET AND WIGGLER

The angular distribution of radiation emitted by electrons following a circular trajectory in a horizontal plane, as in bending magnet, is [5]

$$\frac{d^2F}{d\omega d\Omega} = \frac{3r_e mc^2\gamma^2}{4\pi^2 c}\left(\frac{\omega}{\omega_c}\right)^2\left(1+\gamma^2{\theta_y}^2\right)^2\left[K_{2/3}{}^2(\xi)+\frac{\gamma^2{\theta_y}^2}{1+\gamma^2{\theta_y}^2}K_{1/3}{}^2(\xi)\right], \qquad (1)$$

where ω_c is the critical photon frequency (see below), θ_x and θ_y are the angles of observation in the horizontal and vertical directions (Ω is a solid angle), respectively, r_e and mc^2 are the classical electron radius and electron energy, γ is the Lorentz-factor, K_x are the modified Bessel functions of the second kind, and $\xi \equiv \frac{\omega}{2\omega_c}\left(1+\gamma^2{\theta_y}^2\right)^{3/2}$. The two terms in the last brackets correspond to horizontally and vertically polarized radiation. In the middle plane the second term vanishes, and polarization is purely linear. In other cases both terms contribute, and polarization is elliptical. It is interesting to note that characteristics for two polarization modes differ not only by the intensities but also by the distributions in space. The spatial distribution of the σ-mode is directed mainly in the forward direction, while the π-mode has zero intensity in the plane of electron orbit, $\theta_y = 0$, but emits radiation into two lobes at finite angles.

The energy spectrum from bending magnet is typically smooth and broadband, peaking near, then falling off exponentially above the critical energy $\varepsilon_c \equiv \hbar\omega_c = 3\hbar c\gamma^3/2\rho$, where ρ is

a magnet bending radius. The critical energy and critical wavelength in practical units are given by

$$\varepsilon_c[keV] = 0.665 B[T] E^2[GeV], \qquad \lambda_c\left[\mathring{A}\right] = 18.64 / B[T] E^2[GeV],$$

where B is the bending magnet magnetic field and E is the electron energy.

Wigglers cause electron deflections that are large compared with the natural emission angle of SR, resulting in broadband emission of a fan-shaped beam of photons. It is usual to consider that SR from the wiggler is similar to that produced by an individual bending magnet, but $2N$ times as intense due to repetitive electron bending over the length of a $2N$-pole wiggler:

$$\frac{d^2F}{d\omega d\Omega} = 2N \cdot \frac{3 r_e mc^2 \gamma^2}{4\pi^2 c} \left(\frac{\omega}{\omega_c}\right)^2 \left(1+\gamma^2 {\theta_y}^2\right)^2 \left[{K_{2/3}}^2(\xi) + \frac{\gamma^2 {\theta_y}^2}{1+\gamma^2 {\theta_y}^2} {K_{1/3}}^2(\xi) \right], \qquad (2)$$

where N is a number of wiggler periods, and field strength corresponds to the wiggler field amplitude.

In reality the radiation field structure is formed by interference. It may be more or less smoothed out depending on radiation frequency and on the various effects such as angular acceptance, beam emittance, energy spread and so on.

In a wiggler, radiation from the various periods interferes incoherently. The harmonic peaks are closely spaced that they blur together. Often experimental end stations share the radiation fan of horizontal angular extent $2K/\gamma$, where K is the wiggler strength parameter that defined as ratio between the radiation fan angle and the characteristic radiation cone aperture $1/\gamma$. In practical units we can write a general expression for K

$$K \equiv 0.934 B_0[T] \lambda_w[cm],$$

where B_0 is the wiggler magnetic field and λ_w is the wiggler period. For typical wiggler parameters we have $K>>1$.

The spectral and angular properties of the radiation emitted in wiggler were presented in [6]. Below we briefly describe main features of SR from a wiggler.

The angular distribution of radiation emitted by electrons following a sinusoidal trajectory into the wiggler can be calculated using the equation of the energy radiated per unit bandwidth and per unit solid angle for a relativistic electron with arbitrary trajectory [7]:

$$\frac{d^2F}{d\omega d\Omega} = \frac{3 r_e mc^2}{4\pi^2 c} \cdot \left| \int_{-\infty}^{\infty} \frac{n \times \left[(n-\beta) \times \dot{\beta} \right]}{(1 - n\cdot\beta)^2} \exp\left(i\omega \left(t - \frac{n \cdot r}{c} \right) \right) dt \right|^2, \qquad (3)$$

where $\boldsymbol{n}$ is a unit vector describing the observation direction, $\boldsymbol{r}$, β, $\dot{\beta}$ are the electron position, velocity and acceleration. According to the scheme of Fig.1 the components of $\boldsymbol{n}$ are determined in terms of (θ_x, θ_y) by the following:

$$n_x = \theta_x,\ n_y = \theta_y,\ n_z = 1 - \frac{1}{2}\left(\theta_x^{\,2} + \theta_y^{\,2}\right), \quad \theta_x, \theta_y, \theta_z << 1. \tag{4}$$

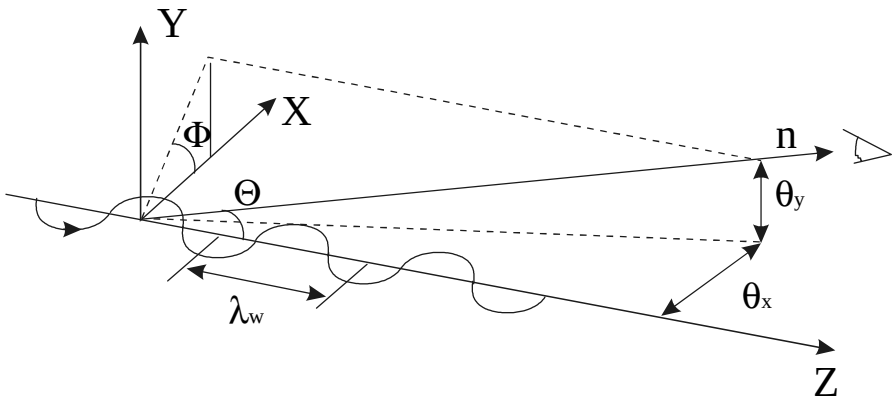

Fig.1. Definition of angles for the SR emission

In the case of a sinusoidal magnetic field variation $B_y = B_0 \cos(k_w z), \quad k_w = \frac{2\pi}{\lambda_w}$ the equations of electron motion in a wiggler are given by [5]:

$$\begin{aligned} x &= \frac{K\lambda_w}{2\pi\gamma}\cos k_w z \\ z &= \left(1 - \frac{K^2}{4\gamma^2}\right)ct + \frac{K^2\lambda_w}{16\pi\gamma^2}\sin 2k_w z \end{aligned} \tag{5}$$

As seen from the scheme of Fig. 2 there are two emission points per period and $\theta_x = -\frac{K}{\gamma}\sin k_w z$.

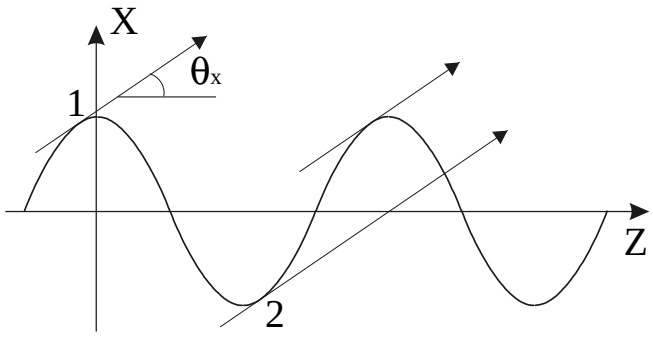

Fig.2. Source points for emission in the horizontal plane

If we define $\alpha = \frac{\gamma\theta_x}{K}$ (the ratio between the horizontal emission angle and the deflection angle of the trajectory), then for two emission points we have:

$$k_w z_1 = -\arcsin\alpha, \quad k_w z_2 = \pi - k_w z_1$$

According to Eq.(3) the equation for the phase of emission can be written as $e^{i\delta}$ - dependence, where $\delta = \omega\left(t - \frac{n \cdot r}{c}\right)$. Substituting expressions (4), and (5), we obtain the following expression

$$\delta = \frac{\omega}{\omega_1}\left(\frac{2\pi z}{\lambda_w}\right) - 2\alpha\frac{K^2}{A}\cos kz - \frac{K^2}{4A}\sin 2kz\,,$$

where $\omega_1 = \frac{2\pi c}{\lambda_w}\cdot\frac{2\gamma^2}{1+\frac{K^2}{2}+\gamma^2\left(\theta_x{}^2+\theta_y{}^2\right)}$ is the wiggler fundamental frequency, and $A = 1+\frac{K^2}{2}+\gamma^2\left(\theta_x{}^2+\theta_y{}^2\right).$

The term in square baskets of Eq.(1) can be rewritten for the wiggler period as follows

$$\left[P_x{}^2 + P_y{}^2\right] = \left(e^{i\delta_1} - e^{i\delta_2}\right)^2 K_{2/3}{}^2(\xi) + \left(e^{i\delta_1} + e^{i\delta_2}\right)^2 \frac{\left(\gamma\theta_y\right)^2}{1+\left(\gamma\theta_y\right)^2} K_{1/3}{}^2(\xi),$$

where P_x, P_y are the amplitudes of polarization in electron orbit plane and in the direction perpendicular to it, δ_1, δ_2 are the phases of two source points. The explanation for the negative sign for P_x and positive for P_y is following. The horizontal component is proportional to $\dot{\beta}_x$. With respect to the nominal point of emission $\dot{\beta}_x$ (and P_x) is symmetric in z and changes in sign depending on the polarity of the wiggler poles. On the other hand, $\dot{\beta}_z$ is antisymmetric and remains the same for all poles. For the combination of two poles the circular polarization rate becomes zero, irrespective of the emission angle.

For the wiggler periods the Eq.(2) can be expressed as a product of the integral and the interference function of the periods $\frac{\sin^2 N\pi\frac{\omega}{\omega_1}}{\sin^2\pi\frac{\omega}{\omega_1}}$. Summing all these expressions results in the final formula for the angular radiation distribution [6, 8]:

$$\frac{d^2F(\omega)}{d\omega d\Omega} = \frac{3r_e mc^2\gamma^2}{4\pi^2 c}\times$$

$$\times\left(\frac{\omega}{\omega_c}\right)^2\left(1+\gamma^2\theta_y{}^2\right)^2 4\left[\sin^2\frac{\Delta}{2}K_{2/3}{}^2(\xi) + \cos^2\frac{\Delta}{2}\frac{\gamma^2\theta_y{}^2}{1+\gamma^2\theta_y{}^2}K_{1/3}{}^2(\xi)\right]\frac{\sin^2 N\pi\frac{\omega}{\omega_1}}{\sin^2\pi\frac{\omega}{\omega_1}}$$

where $\Delta = \frac{\omega}{\omega_1}\left(\pi + 2\arcsin\alpha + 3\frac{K^2}{A}\alpha\sqrt{1-\alpha^2}\right)$. At nonzero horizontal observation angle θ_x, the electron effective radius of curvature at the trajectory locations contributing to the radiation observed, decreases and the off-axis critical energy becomes $\varepsilon_c(\theta_x) = \varepsilon_c(0)\sqrt{1-(\theta_x\gamma/K)^2}$.

The photon flux per unit solid angle into a frequency bin $\frac{\Delta\omega}{\omega}$ and for a circular beam current I is [5]

$$\frac{dN_{ph}}{d\Omega} = \frac{dF}{d\Omega}\cdot\frac{1}{\hbar}\cdot\frac{I}{e}\cdot\frac{\Delta\omega}{\omega}$$

For a wiggler it can be presented in the form below

$$\frac{dN_{ph}}{d\theta_x d\theta_y} = C_\Omega E^2 I\frac{\Delta\omega}{\omega}\left(\frac{\omega}{\omega_c}\right)^2\left(1+\gamma^2\theta_y{}^2\right)^2 4\left[\sin^2\frac{\Delta}{2}K_{2/3}{}^2(\xi) + \cos^2\frac{\Delta}{2}\cdot\frac{\gamma^2\theta_y{}^2}{1+\gamma^2\theta_y{}^2}K_{1/3}{}^2(\xi)\right]\frac{\sin^2 N\pi\frac{\omega}{\omega_1}}{\sin^2\pi\frac{\omega}{\omega_1}}, \quad (6)$$

where $C_\Omega = \frac{1}{137}\frac{3}{4\pi^2 e(mc^2)^2} = 1.3273\cdot 10^{16}$ ph/(sec mrad^2 GeV^2 A).

The factors $\left\{\sin^2\frac{\Delta}{2}, \cos^2\frac{\Delta}{2}\right\}\frac{\sin^2 N\pi\frac{\omega}{\omega_1}}{\sin^2\pi\frac{\omega}{\omega_1}}$ vary fast with respect to the functions $K_{2/3}{}^2(\xi), K_{1/3}{}^2(\xi)$. The maxima and minima of the σ-component and those of the π-component alternate with each other in the spectral distribution: in any given direction we have neighbouring frequencies at which either σ- or π-component is emitted.

The brightness can be approximated by the following expression [9]

$$B = \frac{d\dot{N}/d\theta_x}{(2\pi)^{2/3}\left[\left(\sigma_x{}^2 + a^2 + \sigma_x{}'^2 L^2/12\right)\left(\sigma_y{}^2 + \sigma_y{}'^2 L^2/12\right)\left(\sigma_y{}'^2 + \sigma_R{}'^2\right)\right]^{1/2}}, \quad (7)$$

where $d\dot{N}/d\theta_x$ is the total flux per unit horizontal angle, integrated over the vertical angle, $\sigma_x, \sigma_y, \sigma_x', \sigma_y'$ are the sizes and divergences of electron beam, a is the amplitude of electron sinusoidal motion, L is the wiggler length, σ_R' is the vertical aperture of radiation emitted.

3 THE MAIN PARAMETERS USING IN CALCULATIONS

For calculations of the SR characteristics from DAΦNE bending magnets and wigglers a SynRad computer code [10] was used. This code has been developed at Stanford University and allows us to characterize SR from the bending magnets, wigglers, undulators. Some graphics for illustration of the spectral photon flux in a graph format are accessible. SR from a wiggler is calculated according to Eq. (2). For investigations of the SR interference structure from a wiggler (Eq.(6)) the new computer code is being worked out.

Before calculations the circulating beam parameters were defined. These parameters are presented in Table 1 [1-3].

Table 1. The circulating beam parameters

Energy, MeV	510
Circulating current, A	1.0
Horizontal emittance, m·rad	10^{-6}
Energy spread, %	0.04
Twiss functions at the source point for dipole (for DEAR experiments [11]) β_x, m β_y, m α_x α_y D_x, m D_y, m D_x' D_y'	 5.6 6.16 -2.204 3.6649 1.1053 0 -0.33077 0
Twiss functions at the source point for wiggler (DEAR/KLOE experiments [11]): β_x, m β_y, m α_x α_y D_x, m D_y, m D_x' D_y'	 3.947/2.161 1.191/0.88 -0.089/-1.466 -0.063/-0.2 2.426/1.716 0.0 -0.05/-0.1 0.0
Coupling, %	0.2

The dipole magnet parameters used in calculation are presented in Table 2 [1].

Table 2. The dipole parameters

Type	electromagnet
Bending radius, m	1.4

Magnetic field, T	1.2
Bending angle, rad	0.8
Magnetic rigidity, Tm	1.701

The wiggler parameters used in calculation are presented in Table 3 [11, 12].

Table 3. The wiggler parameters

Type of magnet	Electromagnet
Construction	Rectangular
Magnetic field at the gap center, T	1.8
Number of poles	6
Period length, mm	640
Wiggler length, m	1.92
Gap, mm	40
K-value	107.600

4 SR FROM DAΦNE BENDING MAGNET

According to the data from Tables 1, 2 the sizes and divergences of the electron beam at the source point are the following: σ_x=2407.38 μm, σ_y=111 μm, σ_x'=1031.27 μrad, σ_y'=68.45 μrad. The SR parameters from a dipole magnet are presented in Table 4. Note that all calculations were made for the circulating current of 1A.The angular photon flux, angular and spatial flux density from DAΦNE dipole are presented in Figs. 3, 4. The changes of the angular distribution of radiation for three different frequencies ω are shown in Fig.5. In Table 5 the results of calculation of total flux for both modes of polarization for different observation angles are presented. The expression for the photon fluxes provides the opportunity to calculate the spectral distribution of the photon beam divergence. Photons are emitted into a narrow angle and we may represent this narrow angular distribution by a Gaussian distribution. The effective width of a Gaussian distribution is $\sqrt{2\pi}\sigma_\theta$. The angular divergence of the forward lobe of the photon beam or a beam polarized in the σ-mode is

$$\sigma_\theta(mrad) = \frac{C_\psi}{\sqrt{2\pi}C_\Omega} \cdot \frac{1}{E} \cdot \frac{S(x)}{x^2 K_{2/3}^2(x/2)},$$

where $x = \omega/\omega_c$, $S(x)$ is an universal function of the SR spectrum, $C_\Omega = 1.3273 \cdot 10^{16}$ ph/(s·mrad^2·GeV^2·A), $C_\psi = 3.967 \cdot 10^{19}$ ph/(s·rad·GeV·A). The photon beam divergence for low photon energies compared to the critical photon energy is independent of the particle energy and scales inversely proportional to the cubic root of the bending magnet radius and photon energy. The photon beam divergence from DAΦNE dipole magnet is shown in Fig.6.

Table 4. SR parameters from DAΦNE dipole magnet

Photon critical energy, keV	0.2079
Critical wave length, $\overset{0}{A}$	59.71
Total flux at the critical wave	$8.172 \cdot 10^{12}$

length, ph/(s·mrad·0.1% b.w.)	
Total power, kW	0.5287
Angular power, W/mrad	0.67
Power density at the source point, W/mm^2	1.424

Table 5. Radiated flux into the σ- and π-mode

Vertical observation angle, $\psi\gamma$	Vertical opening angle, mrad	σ-mode, ph/(s·mrad^2)	π-mode, ph/(s·mrad^2)	Total flux, ph/(s·mrad^2)
0.0	0.649	$5.02\cdot10^{12}$	0.0	$5.02\cdot10^{12}$
0.25	0.793	$4.64\cdot10^{12}$	$1.88\cdot10^{11}$	$4.83\cdot10^{12}$
0.5	1.42	$3.60\cdot10^{12}$	$5.25\cdot10^{11}$	$4.12\cdot10^{12}$
0.75	3.59	$2.22\cdot10^{12}$	$6.24\cdot10^{11}$	$2.84\cdot10^{12}$
1	12.9	$1.01\cdot10^{12}$	$4.20\cdot10^{11}$	$1.23\cdot10^{12}$

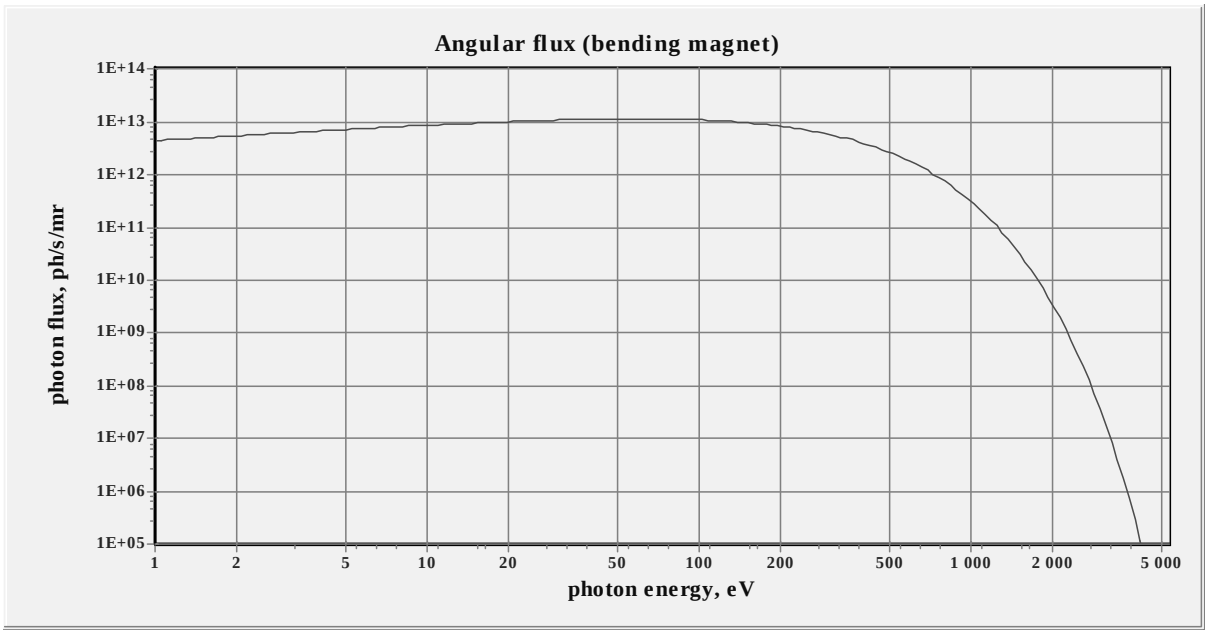

Fig.3. Angular photon flux from DAΦNE dipole magnet

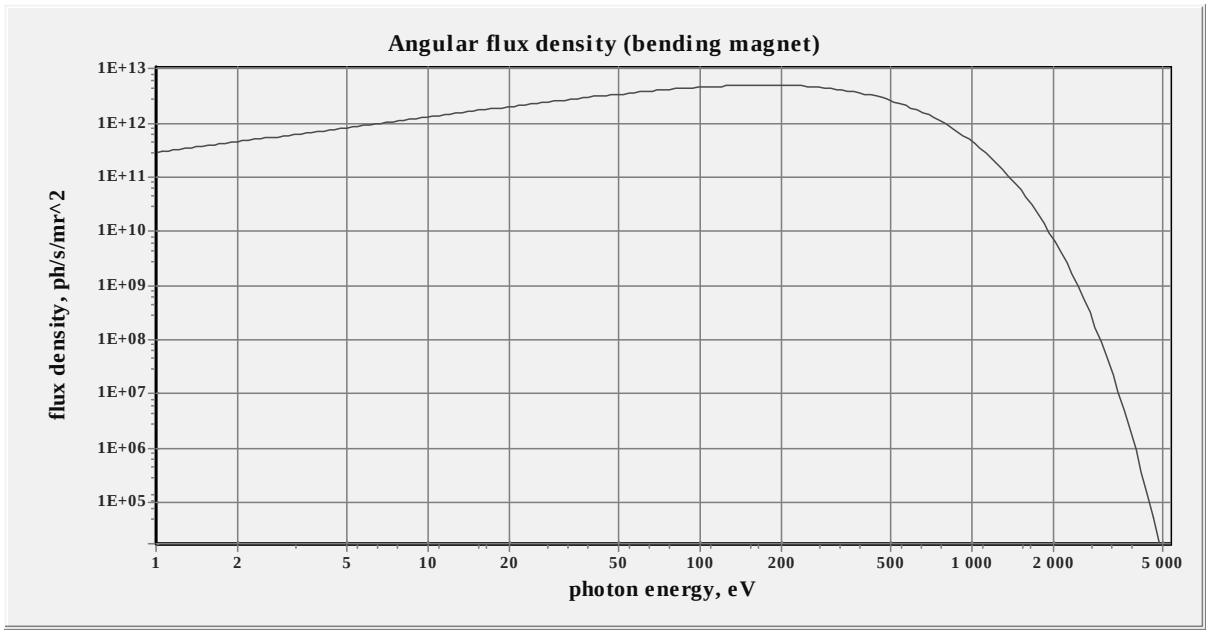

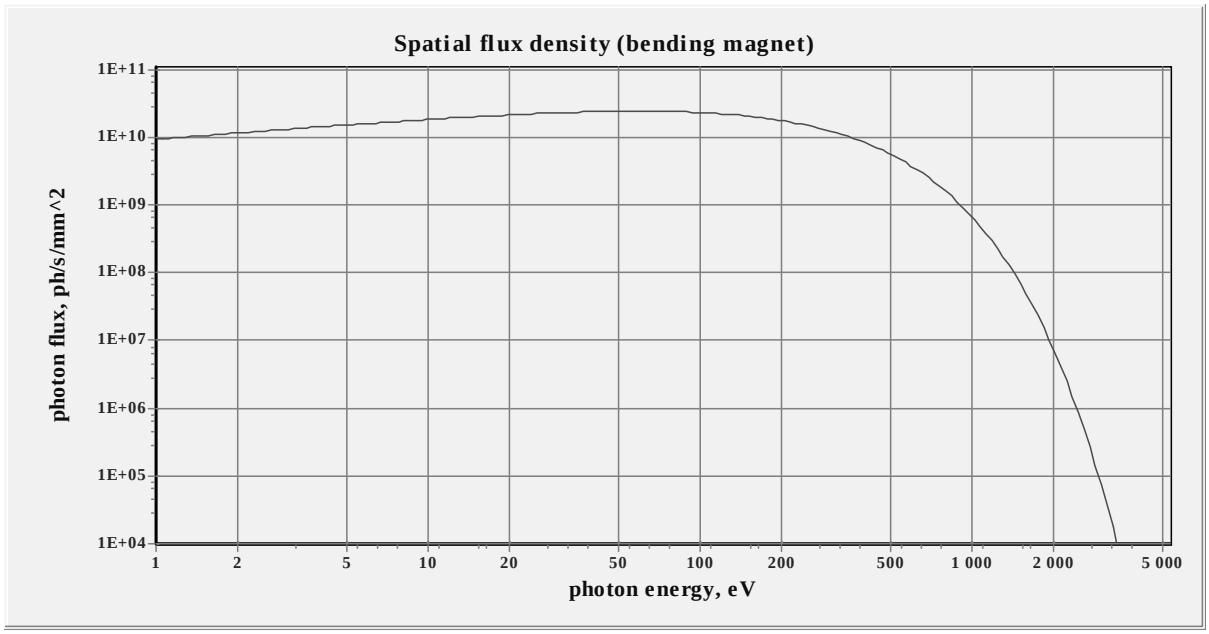

Fig.4. Angular and spatial flux density from DAΦNE dipole magnet

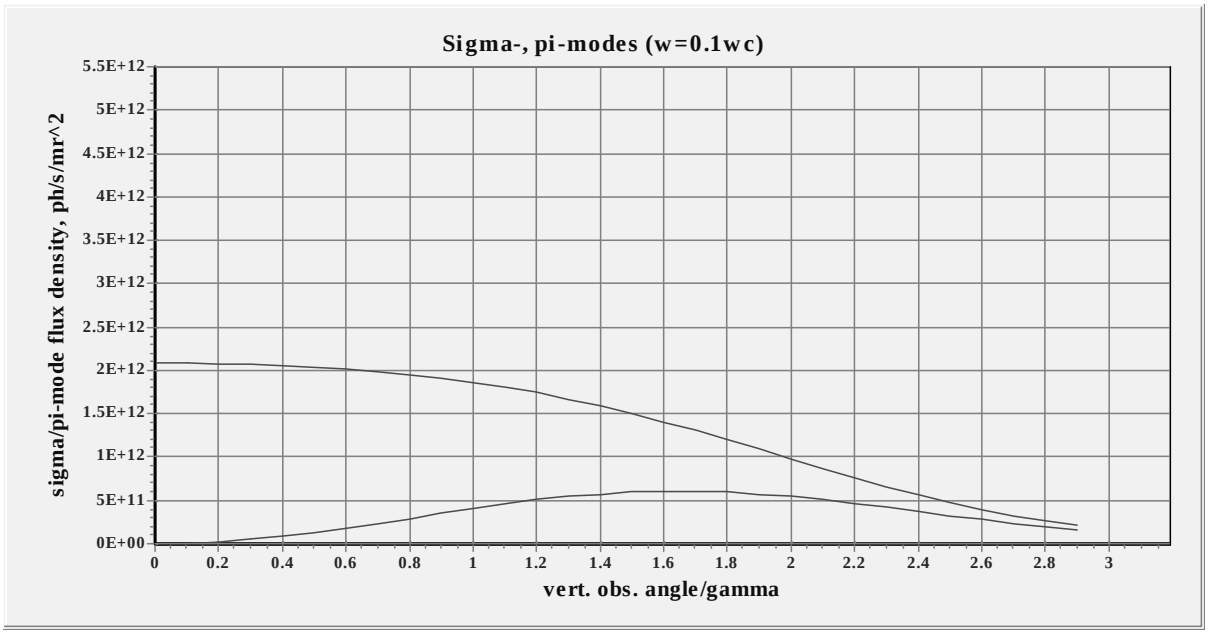
Sigma-, pi-modes (w=0.1wc)
sigma/pi-mode flux density, ph/s/mr^2
5.5E+12
5E+12
4.5E+12
4E+12
3.5E+12
3E+12
2.5E+12
2E+12
1.5E+12
1E+12
5E+11
0E+00
0
0.2
0.4
0.6
0.8
1
1.2
1.4
1.6
1.8
2
2.2
2.4
2.6
2.8
3
vert. obs. angle/gamma

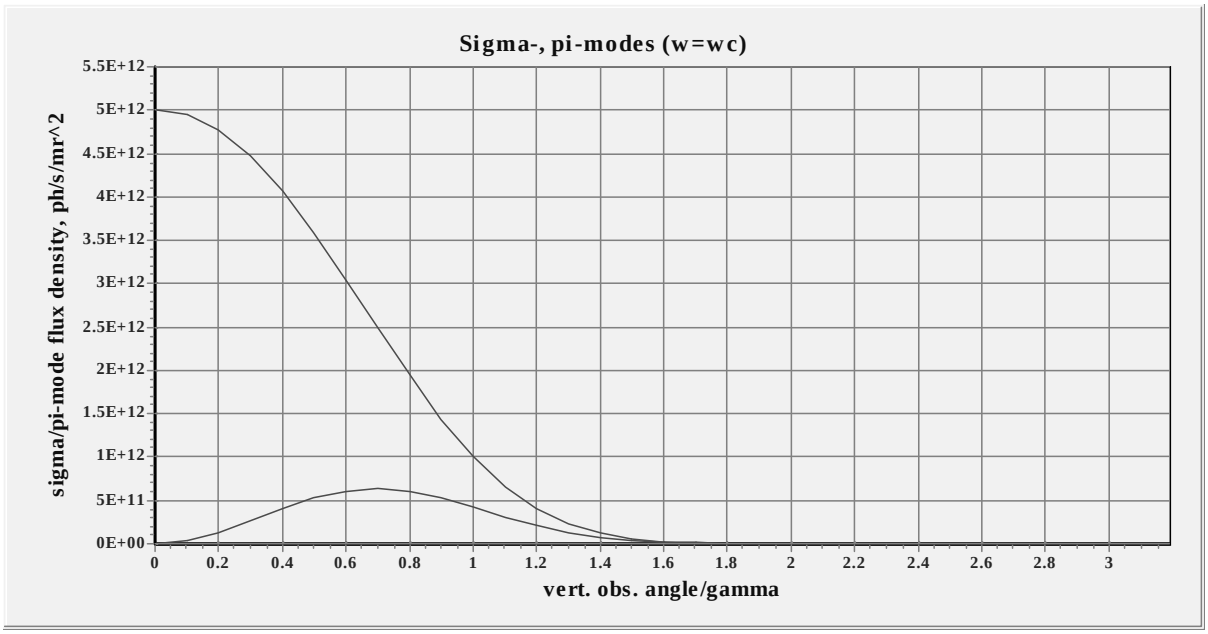
Sigma-, pi-modes (w=wc)
sigma/pi-mode flux density, ph/s/mr^2
5.5E+12
5E+12
4.5E+12
4E+12
3.5E+12
3E+12
2.5E+12
2E+12
1.5E+12
1E+12
5E+11
0E+00
0
0.2
0.4
0.6
0.8
1
1.2
1.4
1.6
1.8
2
2.2
2.4
2.6
2.8
3
vert. obs. angle/gamma

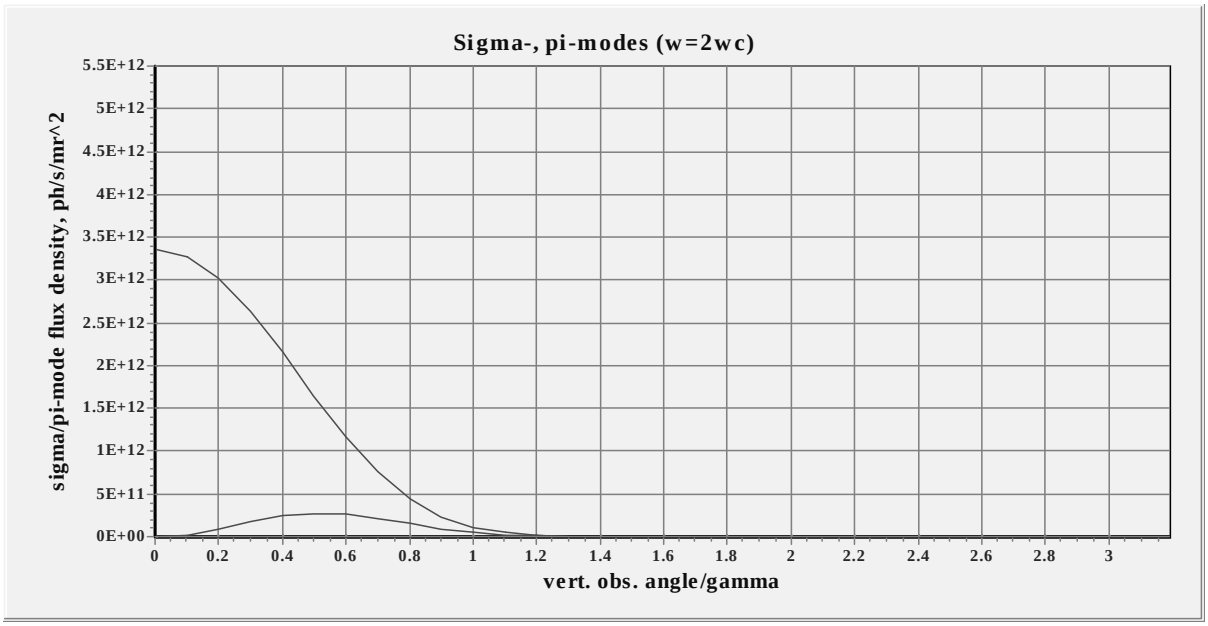

Fig.5. Angular distribution for both modes of polarization at different frequencies $\omega=0.1\omega_c$, ω_c, $2\omega_c$

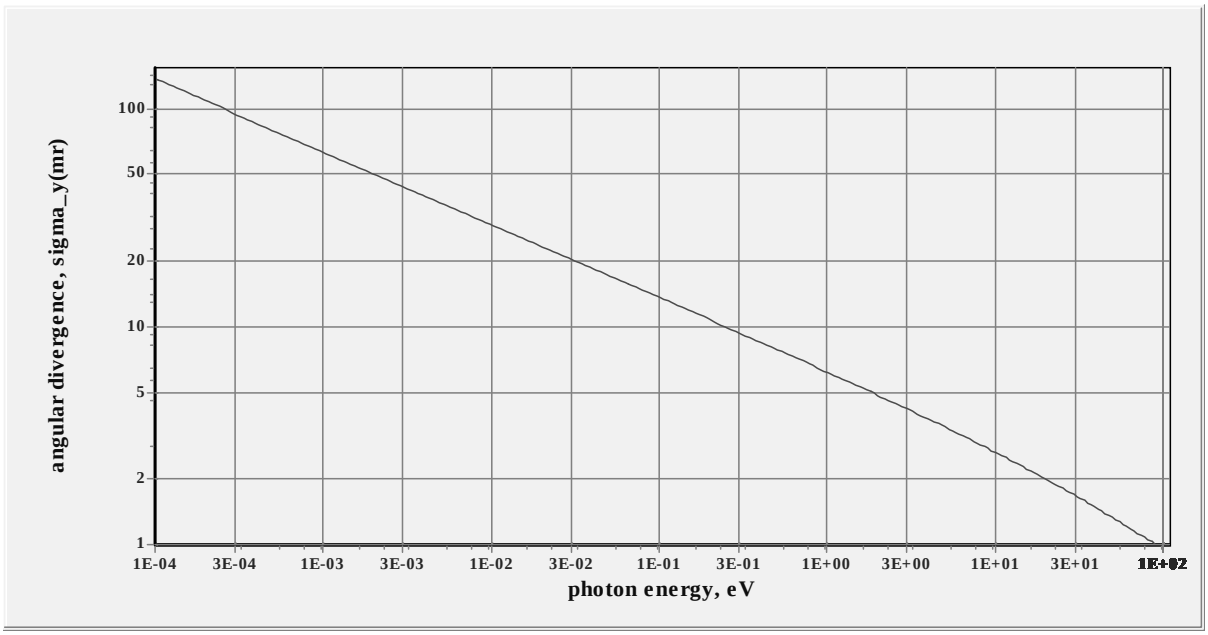

Fig.6. Photon beam divergence from DAΦNE dipole magnet

5 SR FROM DAΦNE WIGGLER

The characteristics of SR from wiggler were calculated for the DEAR experiment. According to data from Table 1, 3 the sizes of the beam at the source point are the followings: σ_x=2211.04 μm, σ_y=48.81 μm, σ_x'=505.73 μrad, σ_y'=41.06 μrad. The maximum path displacement inside the wiggler is 21.97 mm, the maximum angle deflection is 107.9 mrad.

The characteristics of SR beam parameters from the DAΦNE wiggler (circulating current of 1 A) using the parameters for the DEAR experiment are presented in Table 6.

Table 6. SR parameters from the DAΦNE wiggler

Photon critical energy, keV	0.31134
Critical wave length, $\overset{0}{A}$	39.823
Vertical cone, μrad	650
Angular flux for the critical wave length, ph/(s·mrad·0.1% b.w.)	$4.90 \cdot 10^{13}$
Flux density at the critical wave length, ph/(s·mrad^2·0.1% b.w.)	$3.01 \cdot 10^{13}$
Brightness at the critical wave length, ph/(s·mm^2·mrad^2·0.1% b.w.)	$4.44 \cdot 10^{7}$
Total radiation power, kW	1.025
Power density at the source point, kW/mm^2	1.512

The angular photon flux produced by the DAΦNE wiggler is presented in Fig. 7. In Fig. 8, 9 the angular flux density and spatial flux density are shown.

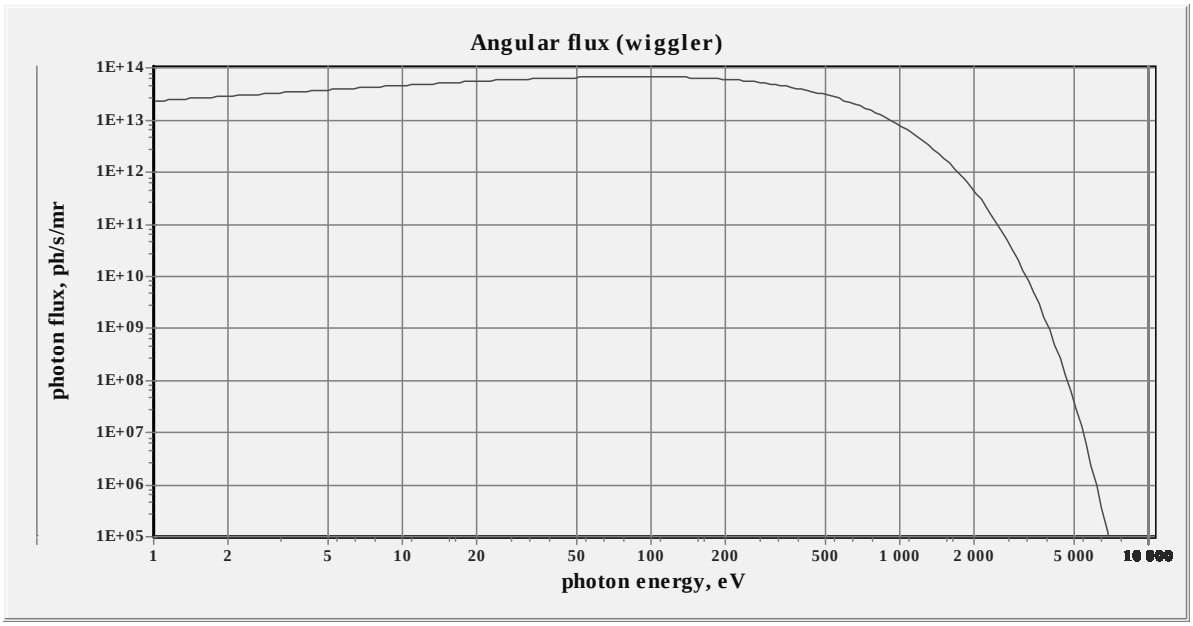

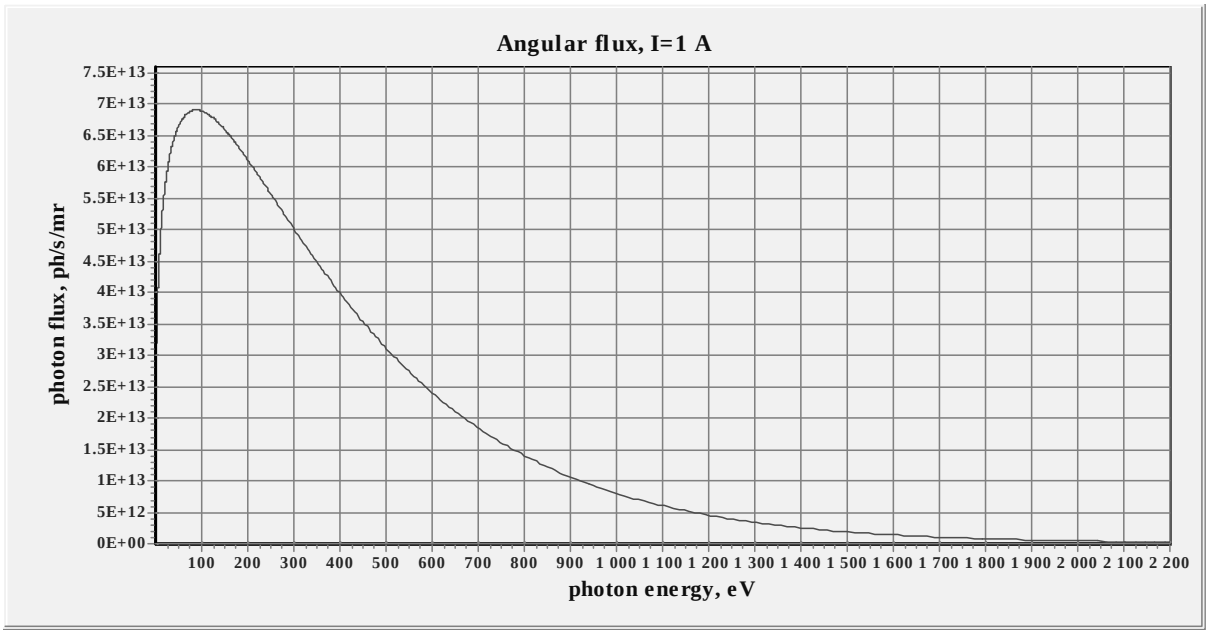

Fig.7. Angular flux from the DAΦNE wiggler in log and linear scales

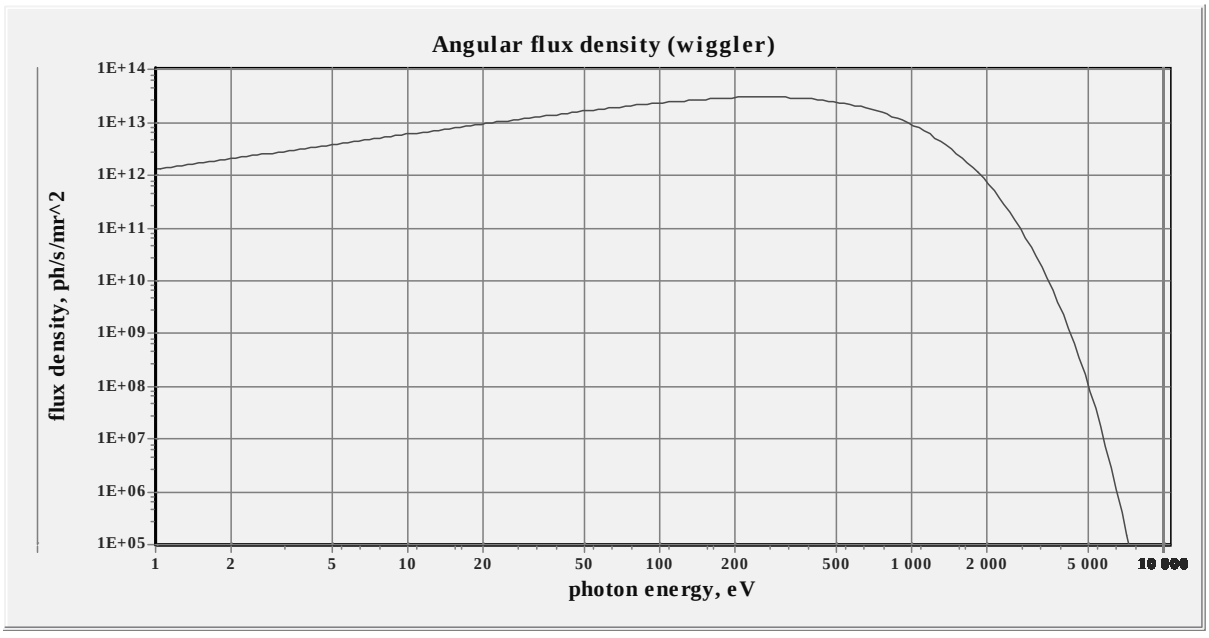

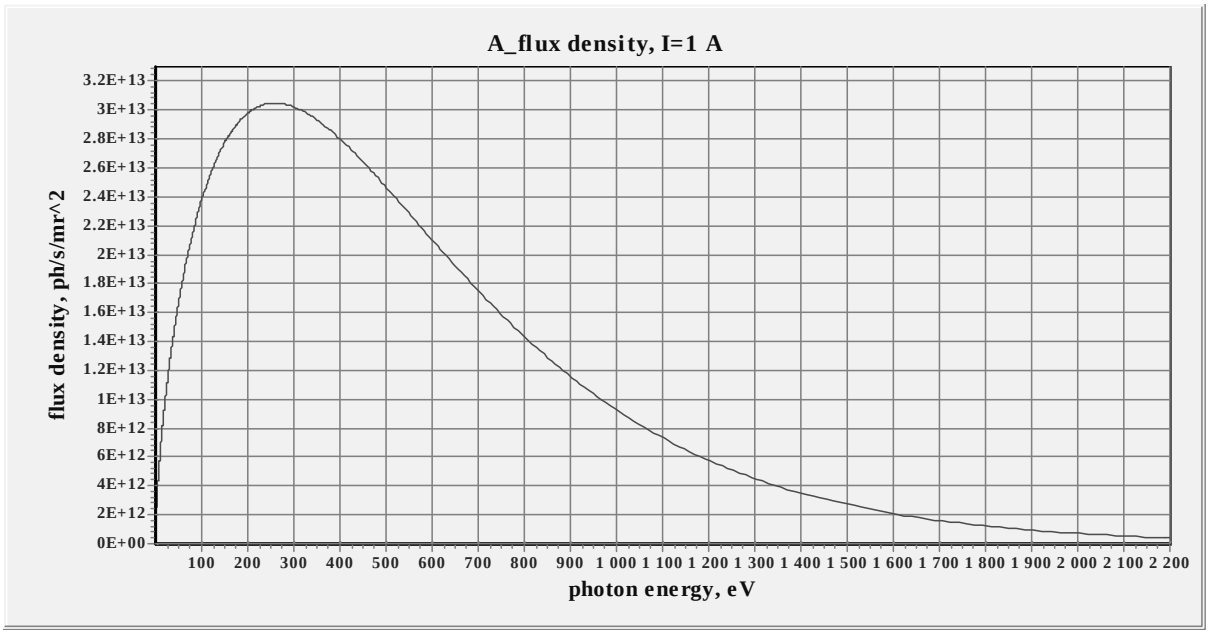

Fig.8. Angular flux density from the DAΦNE wiggler in log and linear scales

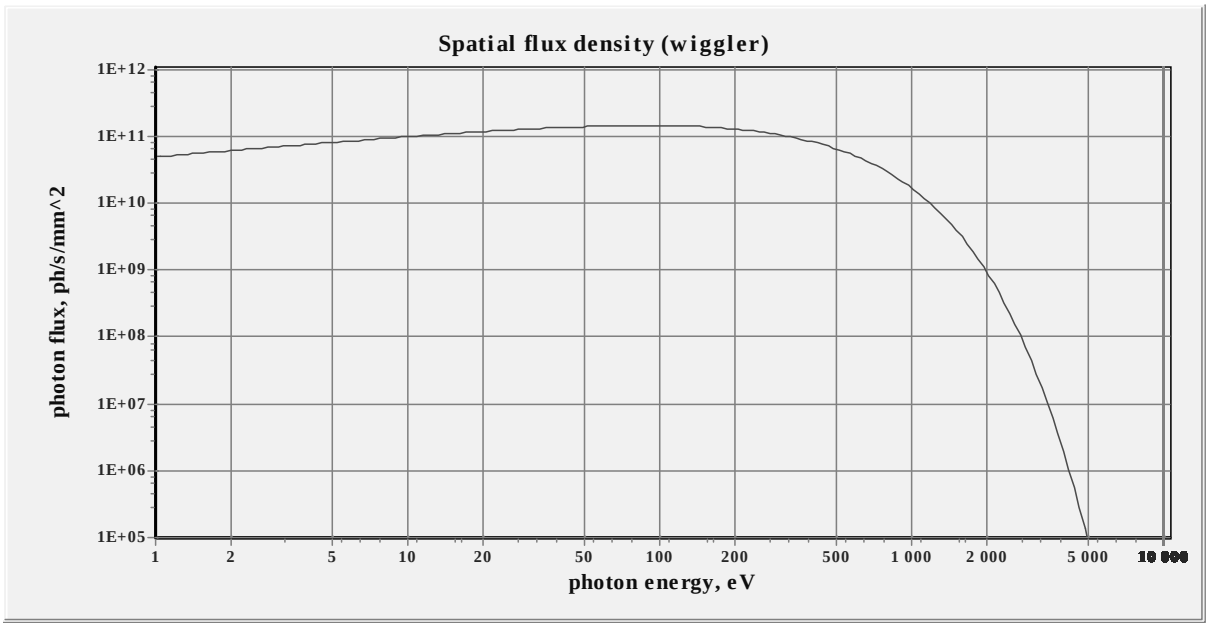

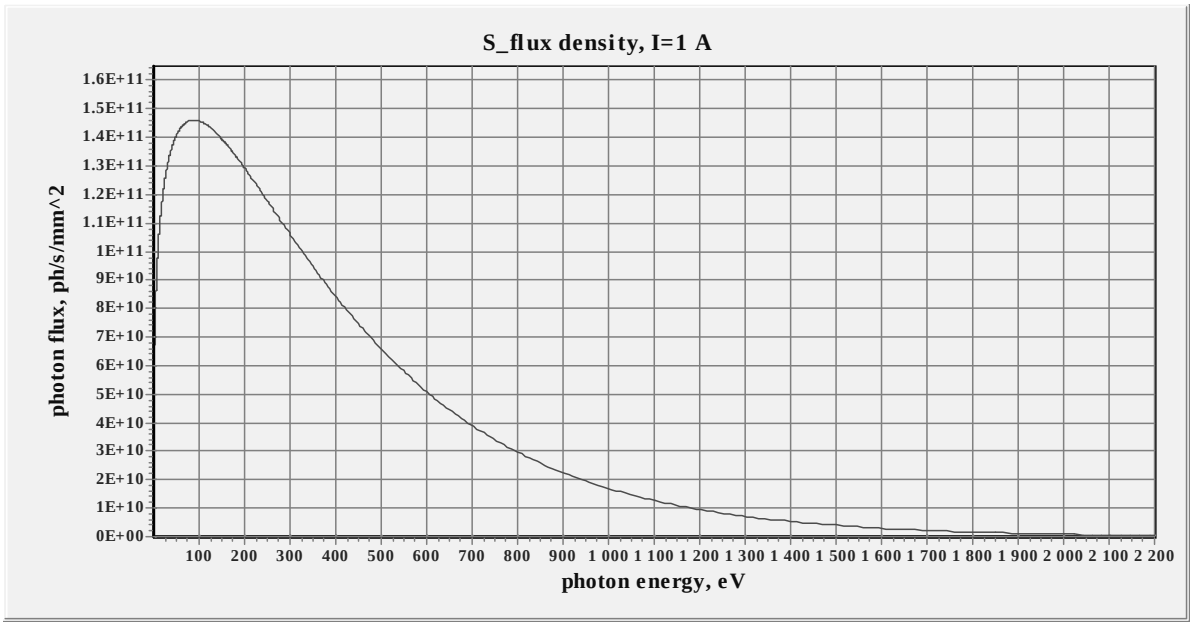

Fig.9. Spatial flux density from the DAΦNE wiggler in log and linear scales

According to Eq. (2) the angular flux density for the plate of 15×4 mm^2 placed in the X-ray beam was calculated. The distance between the wiggler and the plate is 18 m. These dimensions correspond to the angular sizes of the plate, $\theta_x = 53.086 \div 53.914$ mrad, $\theta_y = 0 \div 0.222$ mrad. The results of calculations for the radiation with critical wavelength are presented in Fig. 10. The maximum flux density is $2.9208 \cdot 10^{13}$ ph/(s·mrad^2), the minimum equals to $2.8038 \cdot 10^{13}$ ph/(s·mrad^2).

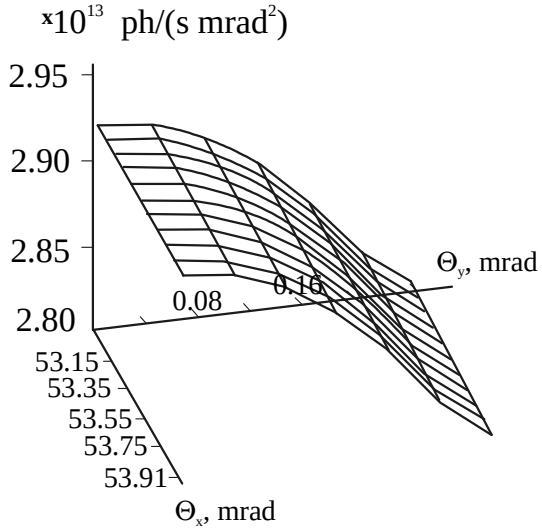

Fig.10. Angular flux density for the plate in the X-ray beam

According to Eq. (7) the brightness of wiggler's radiation depends on size and divergence of the electron beam. In Fig. 11 the brightness for two wiggler regimes is shown, the Twiss-parameters in this calculation correspond to the KLOE and DEAR experiments. As seen from the graphs, the KLOE regime provides more brightness then the DEAR one.

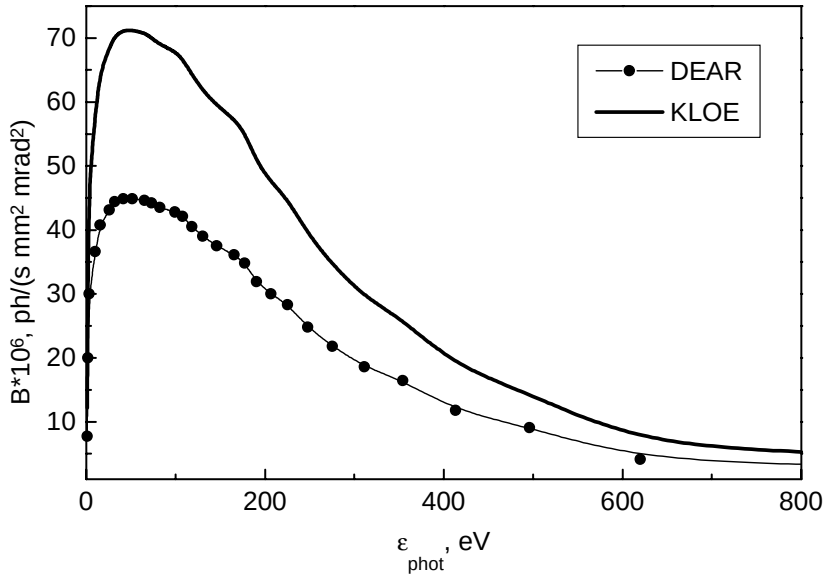

Fig.11. Brightness from the wiggler for two operation regimes

6 CONCLUSION

In this paper the main characteristics of SR for the Main Ring dipole magnet and wiggler are presented. The angular photon flux, photon beam divergence for SR from dipole magnet, and the angular flux and angular/spatial flux density of SR from wiggler are calculated. The angular flux density of SR on the plate placed in X-ray beamline is evaluated. All these calculations were based on the SynRad computer code. This code doesn't take into account the interference structure of radiation from a wiggler. Typically the radiation spectra from a wiggler are smoothed by spatial and angular variables, however, for specific cases to count a residual interference structure can resolve some important features. That's why new computer code taking into account an interference effect is worked out.

The brightness of SR for two regimes of the Main Ring operation is calculated. It is shown that for high brightness of SR the KLOE regime is preferable.

To obtain the better parameters of SR from wiggler the detailed analysis of lattice function is needed. The optimisation of the Main Ring optics for good conditions of high-energy experiments as well as for good parameters of wiggler's SR is the next step, and will be discussed separately in the subsequent paper.

7 REFERENCES

[1] M.E. Biagini, "DAΦNE Status Report", *Proc. of EPAC'92*, p.60

[2] M.E. Biagini, S. Guiducci et al, "DAΦNE Lattice Update", *Proc. of EPAC'92*, p.424.

[3] M. Bassetti, M.E. Biagini et al., "DAΦNE Main Ring Optics", *Proc. of EPAC'98*, p.879.

[4] M. Bassetti, *Proc. of V Int. Conference on High Energy Accelerators*, p.709.
[5] H. Wiedemann, “Particle Accelerator Physics”, v.2, Springer-Verlag 1993.
[6] R.P. Walker, “Interference Effect in Undulator and Wiggler Radiation Sources”, *Nucl. Instr. Meth.* **A335** (1993) 328-337.
[7] J.D. Jackson, “Classical Electrodynamics”, 1975, p.674.
[8] V.Ya. Epp, G.K. Razina, “Radiation in a Wiggler with /sinusoidal Magnetic Field”, *Nucl. Instr. Meth.* **A307**(1991) 562-567.
[9] R.P. Walker, SST/M-TN-89/24, July 1989.
[10] http://coherent.stanford.edu/He-Web/PC-programs.html
[11] S. Sanelli, H. Hsieh, “Design of the 1.8 Tsla Wiggler for the DAΦNE Main Rings”, *Proc. of EPAC’92*, p.1391.
[12] H. Hsieh, M. Modena et al, “The 1.8 Tesla Wiggler for the Main Rings of DAΦNE, the Frascati Φ-Factory”, *Proc. of EPAC’94*, p.2247.